time of gas in the cell. (2) The size of the clusters correlates with disilane partial pressure, higher partial pressures resulting in larger clusters and vice versa. (3) The average size of the particles does not change noticeably as a function of laser repetition rate, over the range 0.7–12.8 Hz. (4) No clusters are observed on the grids if the photolysis is carried out in the absence of disilane. (5) The crystalline clusters were typically in the 3–10-nm size range. No further characterization of the size distribution was possible since the larger area microscope images did not have suitable contrast to be digitized and analyzed. Observation 1 suggests that the clusters initially grow as amorphous material in the gas phase following a single laser pulse and are annealed and crystallized in the gas phase by subsequent laser pulses. Observation 2 is consistent with the growth being from gas-phase intermediates and/or adsorption of disilane onto the surface of nucleated clusters. Observation 3 supports the contention that the clusters grow as the result of a single laser pulse. If growth were the result of repeated pulses, then higher laser repetition rates should lead to larger and larger clusters. This is not observed. Observation 4 serves as a control and rules out laser sputtering of material from cell windows, walls, or the substrate holder as the source of clusters. The detailed growth mechanism of the clusters remains to be studied, and it is possible that the process is more complicated than that suggested above. It is important to note, however, that the disilane partial pressure has the most pronounced effect on cluster size and the laser repetition rate, relative to the average residence time of clusters in the cell, has the most pronounced effect on cluster morphology. The TEM samples were routinely handled and transported in air. They were stored in a nitrogen-purged desiccator for periods of weeks and were shown to remain crystalline by electron diffraction.

Several bulk samples were also prepared. Qualitatively, these samples have an optical gap similar to that of microcrystalline silicon and an infrared spectrum which resembles that of a heavily hydrogenated phase.[14] The samples were transparent adherent films with a yellowish color. The UV–vis spectrum of one such sample was obtained by scraping the material off a glass substrate and suspending the sample in ethanol. From this spectrum, an optical gap of 1.8 eV was determined from a plot of $(\alpha E)^{1/2}$ vs E, where α is the optical density and E is the photon energy (Tauc plot).[5,15] The infrared spectrum of the samples, obtained on a NaCl substrate, indicates that hydrogen is present. The strongest bands occur at 2100, 1250, 910, and 870 cm^{-1}. With the exception of the band at 1250 cm^{-1}, the remaining bands correspond reasonably well to those assigned to SiH$_2$ and/or SiH$_3$ groups in the hydrogenated silicon literature. It is possible that the 1250 cm^{-1} is the first overtone of a strong SiH$_x$ mode which is normally seen at 630 cm^{-1} and is just at the cutoff of the NaCl substrate. No X-ray diffraction pattern above background could be observed from any of the bulk samples. One such sample was scraped from the substrate following the diffraction scan, taken up in ethanol, dropped onto a TEM grid and examined. The sample showed a strongly crystalline electron diffraction pattern and the presence of nanocrystals. The bulk samples oxidized slowly over the course of a few days in air as evidenced by the appearance of a strong SiO stretching band at ≃1080 cm^{-1} in the FTIR spectrum.[14,15] While the TEM results provide unequivocal evidence that crystalline nanoclusters

are produced, the results for the bulk samples suggest that a substantial amount of heavily hydrogenated amorphous material may also be present.

In conclusion, we have demonstrated that crystalline silicon nanoclusters are formed in the gas-phase laser photolysis of disilane dilute in helium at room temperature. The experiments strongly suggest that the clusters grow as amorphous material which is annealed and crystallized in the gas phase by subsequent laser pulses. This represents a rational photochemical synthesis of silicon nanoclusters. Further work is clearly required to determine the factors which most strongly control the average cluster size and the size distribution, as well as to accurately characterize the bulk samples. Finally, we note that the photochemical method described above should be compatible with the preparation of n-type and p-type doped nanoclusters by cophotolysis of phosphine, arsine, or diborane,[16] the preparation of germanium nanoclusters by photolysis of digermane,[17] and the preparation of silicon–germanium alloys by cophotolysis of disilane and digermane.

(16) Clark, J. H.; Anderson, R. G. *Appl. Phys. Lett.* **1978**, *32*, 46.
(17) Eres, D.; Lowndes, D. H.; Tischler, J. Z.; Sharp, J. W.; Geohegan, D. B.; Pennycook, S. J. *Mater. Res. Soc. Symp. Proc.* **1989**, *131*, 517.

Intercalation of Poly(ethylene oxide) in V$_2$O$_5$ Xerogel

Y.-J. Liu,[†] D. C. DeGroot,[‡] J. L. Schindler,[‡] C. R. Kannewurf,[‡] and M. G. Kanatzidis*,[†]

Department of Chemistry and Center of Fundamental Materials Research Michigan State University East Lansing, Michigan 48824 Department of Electrical Engineering and Computer Science Northwestern University, Evanston, Illinois 60208

V$_2$O$_5$·nH$_2$O is a porous solid with a layered structure, and it is capable of diverse intercalation chemistry.[1] This material can be easily fabricated into films and coatings and can act as a host lattice by accepting neutral or charged guest species.[2–4] Intercalation can involve cation

† Michigan State University.
‡ Northwestern University.

(1) (a) Lemerle, J.; Nejem, L.; Lefebvre, J. *J. Inorg. Nucl. Chem.* **1980**, *42*, 17–20. (b) Bullot, J.; Gallais, O.; Gauthier, M.; Livage, J. *Appl. Phys. Lett.* **1980**, *36*, 986–988. (c) Sanchez, C.; Babonneau, F.; Morineau, R.; Livage, J.; Bullot, J. *Philos. Mag., Part B* **1983**, *47*, 279–290.
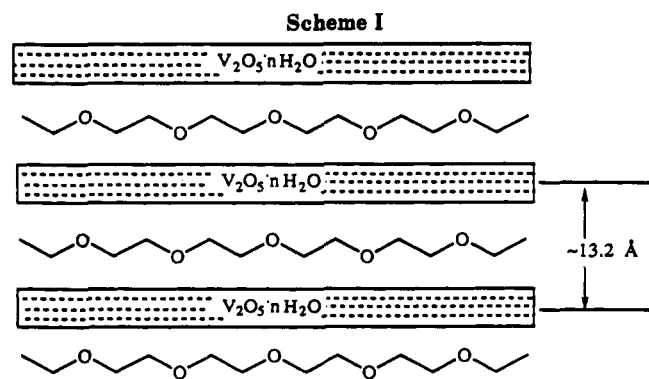(2) (a) Legendre, J.-J.; Livage, J. *J. Colloid Interface Sci.* **1983**, *94*, 75–83. (b) Legendre, J. J.; Aldebert, P.; Baffier, N.; Livage, J. *J. Colloid Interface Sci.* **1983**, *94*, 84–89. (c) Aldebert, P.; Haesslin, H. W.; Baffier, N.; Livage, J. *J. Colloid Interface Sci.* **1983**, *98*, 478–483. (d) Gharbi, N.; Sanchez, C.; Livage, J.; Lemerle, J.; Nejem, L.; Lefebvre, J. *Inorg. Chem.* **1982**, *21*, 2758–2765.
(3) (a) Aldebert, P.; Baffier, N.; Legendre, J.-J.; Livage, J. *Rev. Chim. Miner.* **1982**, *19*, 485–495. (b) Lemordant, D.; Bouhaouss, A.; Aldebert, P.; Baffier, N. *J. Chim. Phys.* **1986**, *83*, 105–113. (c) Aldebert, P.; Baffier, N.; Gharbi, N.; Livage, J. *Mater. Res. Bull.* **1981**, *16*, 949–955.
(4) Livage, J. *J. Solid State Chem.* **1986**, *64*, 322–330.

(14) *Properties of Amorphous Silicon*; EMIS Datareviews Series No. 1; Institute of Electrical Engineers: Surrey, England, 1985.
(15) Richter, H.; Ley, L. *J. Appl. Phys.* **1981**, *52*, 7281.

Communications

Chem. Mater., Vol. 3, No. 6, 1991 993

Scheme I

Figure 1. X-ray diffraction pattern from $(PEO)_{0.50}V_2H_5 \cdot 1.60H_2O$ film at low water pressure.

exchange, acid–base, coordination, and redox reactions. The first two types have been explored in more detail.[3,5] Redox intercalation alters the host's band structure forming bronzelike materials with enhanced electrical properties.[6] During the past few years we have investigated in detail the redox intercalation properties of this host, particularly the intercalative redox polymerization of several organic molecules such as aniline, pyrrole, and 2,2'-bithiophene.[7] The conductive polymer containing products are highly conductive mixed-valence $V^{4+/5+}$ compounds. Recently, we extended our interests to the intercalation of insulating polymers as well. Here we report the synthesis and properties of a new class of intercalation compounds [poly(ethylene oxide)]$_x$V$_2$O$_5 \cdot n$H$_2$O. We chose poly(ethylene oxide) (PEO) because its complexes with alkali-metal ions have been studied extensively as solid electrolytes.[8] Various PEO/alkali-metal salt complexes are promising for applications in all-solid-state batteries and electrochromics.[8] Since $V_2O_5 \cdot n$H$_2$O displays interesting reversible battery cathode and electrochromic properties associated with alkali-metal ion (primarily Li$^+$) intercalation into its structure,[9] PEO/V$_2$O$_5 \cdot n$H$_2$O intercalation compounds are worthy of investigation. Such systems could display Li$^+$ intercalation in which PEO–Li$^+$ interactions could be studied inside the constrained host structure of V$_2$O$_5 \cdot n$H$_2$O.

The synthesis of the new PEO/V$_2$O$_5 \cdot n$H$_2$O compounds is facile and is accomplished by simply mixing aqueous solutions of PEO[10] with aqueous gels of vanadium oxide
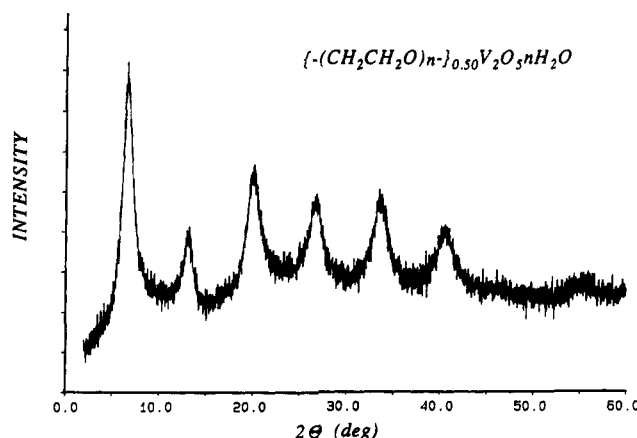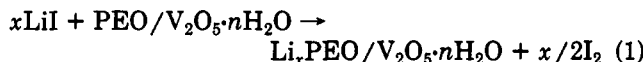
in various ratios. Slow evaporation of water yields a layered hydrated PEO/V$_2$O$_5$ red-colored composite with an interlayer spacing of 13.2 Å. The net intralayer distance associated with this spacing is 4.5 Å and indicates a straight-chain conformation for the PEO (rather than coiled), as shown in Scheme I. Single-phase products were obtained when the PEO/V$_2$O$_5 \cdot n$H$_2$O ratio was less than 0.8. At higher ratios a second phase appears with an interlayer spacing of 16.5 Å. The PEO/V$_2$O$_5 \cdot n$H$_2$O compounds are swellable in water, and they can be cast into flexible thin films. PEO/V$_2$O$_5 \cdot n$H$_2$O films can absorb water reversibly depending on the water partial pressure. This can be seen easily via changes in the X-ray diffraction pattern, which shows a decrease (1.6 Å) in the interlayer spacing and a noticeable sharpening of the diffraction lines on a low water pressure; see Figure 1. When the PEO/ V$_2$O$_5 \cdot n$H$_2$O films are dried in air, typical values of n range from 1.6 to 1.8. Furthermore, we noticed that free-standing PEO/V$_2$O$_5 \cdot n$H$_2$O films exhibit improved mechanical flexibility compared to the V$_2$O$_5 \cdot n$H$_2$O films.

The PEO/V$_2$O$_5 \cdot n$H$_2$O films are also capable of ion redox intercalation. For example, Li$^+$ could be intercalated in the material by reaction with LiI according to eq 1. No

$$x\text{LiI} + \text{PEO}/\text{V}_2\text{O}_5 \cdot n\text{H}_2\text{O} \rightarrow$$
$$\text{Li}_x\text{PEO}/\text{V}_2\text{O}_5 \cdot n\text{H}_2\text{O} + x/2\text{I}_2 \quad (1)$$

iodine was detected in the products by electron microprobe analysis. The interlayer distance of the product is 13.0 Å. The dark-blue bronzelike compounds are significantly more conductive than the pristine counterparts. We are currently exploring the complexation properties of the intercalated PEO towards Li$^+$. A variety of ions might be intercalated in a similar fashion.

Interestingly, we found that (PEO)$_x$V$_2$O$_5 \cdot n$H$_2$O films are light sensitive and turn dark blue upon standing in room light for several weeks. Exposure to a medium-pressure Hg lamp filtered by Pyrex glass causes the materials to turn blue in several hours. This color change is due to a light-induced redox reaction in which the PEO presumably is oxidized by the vanadium oxide framework. PEO films themselves are also light sensitive but on a much longer time scale.[11] Pristine V$_2$O$_5 \cdot n$H$_2$O films are not light sensitive. We have not yet identified the oxidation product of PEO, as infrared spectroscopy shows no significant changes in the PEO vibration spectrum before and after irradiation for at least 18 h. In addition, we do not observe obvious changes in the position and shape of the stretching

(5) Bouhaouss, A.; Aldebert, P. *Mater. Res. Bull* **1983**, *18*, 1247–1256.

(6) (a) Masbah, H.; Tinet, D.; Crespin, M.; Erre, R.; Setton, R.; Van Damme, H. *J. Chem. Soc., Chem. Commun.* **1985**, 935–936. (b) Van Damme, H.; Lettellier, M.; Tinet, D.; Kihal, B.; Erre, R. *Mater. Res. Bull.* **1984**, *19*, 1635–1642. (c) Babonneau, F.; Barboux, P.; Josien, F. A.; Livage, J. *J. Chim. Phys.* **1985**, *82*, 761–766. (d) Murphy, D. W.; Christian, P. A.; DiSalvo, F. J.; Waszczak, J. V. *Inorg. Chem.* **1979**, *18*, 2800–2803. (e) Wu, C.-G.; Kanatzidis, M. G.; Marcy, H. O.; Kannewurf, C. R. Manuscript in preparation.

(7) (a) Kanatzidis, M. G.; Wu, C.-G.; Marcy, H. O.; Kannewurf, C. R. *J. Am. Chem. Soc.* **1989**, *111*, 4139–4141. (b) Wu, C.-G.; Kanatzidis, M. G.; Marcy, H. O.; DeGroot, D. C.; Kannewurf, C. R. *Polym. Mater. Sci. Eng.* **1989**, *61*, 969–973. (c) Wu, C.-G.; Kanatzidis, M. G.; Marcy, H. O.; DeGroot, D. C.; Kannewurf, C. R. *NATO Advanced Study Institute; Lower Dimensional Systems and Molecular Devices*; Metzger, R. M., Ed. Plenum Press: New York, 1991; pp 427–434. (d) Wu, C.-G.; Kanatzidis, M. G. Symposium on *Solid State Ionics II*; Nazri, G., Huggins, R. A., Shriver, D. F., Balkanski, M., Eds.; *MRS Symp. Proc.* **1991**, *210*, 429–442.

(8) (a) Ratner, M. A.; Shriver, D. F. *Chem. Rev.* **1988**, *88*, 109–124. (b) *Solid State Ionics*; Nazri, G., Huggins, R. A., Shriver, D. F., Eds.; *MRS Symp. Proc.* **1989**, *135*. (c) *Solid State Ionics II*; Nazri, G., Huggins, R. A., Shriver, D. F., Balkanski, M., Eds.; *MRS Symp. Proc.* **1991**, *210*. (d) Armand, M. B.; Chabango, J. M.; Duclot, M. J. In *Fast Ion Transport in Solids*; Vashista, P., Mundi, J. N., Shenoy, G. K. Eds.; North-Holland: New York, 1979, p 131. (e) *Polymer Electrolyte Reviews* McCallum, J. R., Vincent, C. A., Eds.; Elsevier Applied Science: London, 1987 and 1989 Vols. 1, 2. (f) Armand, M. *Annu. Rev. Mater. Sci.* **1986**, *16*, 245.

(9) Livage, J. *Chem. Mater.* **1991**, *3*, 578–593.

(10) PEO of various molecular weight was used with similar results. The work reported here was carried out primarily with PEO of mw of 100 000.

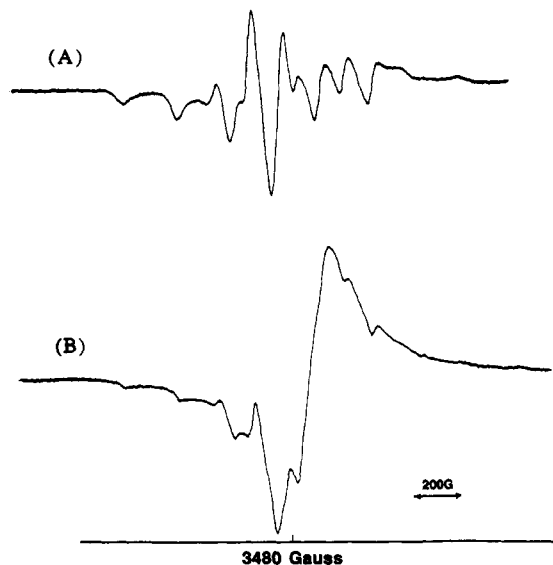(11) McGary, C. W. Jr. *J. Polym. Sci.* **1960**, *46*, 51–57.

994 *Chem. Mater., Vol. 3, No. 6, 1991*

Communications

Figure 2. (A) EPR spectrum of freshly prepared $(PEO)_{0.50}V_2O_5 \cdot nH_2O$ ($n \sim 1.6$–1.8). A few unpaired spins are always present due to some unavoidable reduction of V^{5+} during preparation of $V_2O_5 \cdot nH_2O$ xerogel.[9] (B) EPR spectrum of irradiated $(PEO)_{0.50}V_2O_5 \cdot nH_2O$. Irradiation time was 18 h. The spectra were recorded at room temperature.

vibration peaks of the vanadium oxide framework (at 1014, 750, 496 cm^{-1}, respectively), suggesting that no structural changes are occurring in the framework.

The redox nature of this transformation is confirmed readily by EPR spectroscopy. The EPR signal of irradiated samples increases in intensity with irradiation time due to the increased concentration of V^{4+} centers. This is accompanied with a gradual disappearance of the original hyperfine splitting pattern arising from the ^{51}V ($I = {}^{7}/_2$) nucleus. Figure 2 shows the changes in the EPR spectra upon irradiation. The increase in spin concentration in the irradiated samples is also apparent in the magnetic susceptibility data, which follow Curie–Weiss law behavior and show a significant enhancement of the magnetic moment to values, at 300 K, corresponding to 0.8 μ_B per formula unit.

The irradiated samples have dramatically different properties including enhanced conductivity and diminished solubility.[12] The enhanced conductivity (10^{-2} S/cm at room temperature) is rationalized on the basis of increased carrier (spin) concentration in the vanadium oxide framework. A variable temperature conductivity plot of an irradiated $(PEO)_{0.50}V_2O_5 \cdot nH_2O$ and a sample before irradiation are shown in Figure 3A. They clearly indicate nearly 2 orders of magnitude increase in conductivity. The temperature dependence suggests semiconducting character. Interestingly, the activation energy calculated from these data for both samples is similar at 0.24 eV. This may be a consequence of the fact that only minimal structural changes occur in the vanadium oxide framework. The paramagnetic behavior of irradiated $(PEO)_{0.50}V_2O_5 \cdot nH_2O$ and the conductivity data suggest that these materials are small polaron conductors (localized but mobile electronic spins). This is confirmed by the thermoelectric power data which show negative Seebeck coefficients of -140 mV/K at 300 K which decreases with temperature. The Seebeck coefficient of the irradiated samples is considerably less negative than their precursor $(PEO)_{0.50}V_2O_5 \cdot nH_2O$ samples,

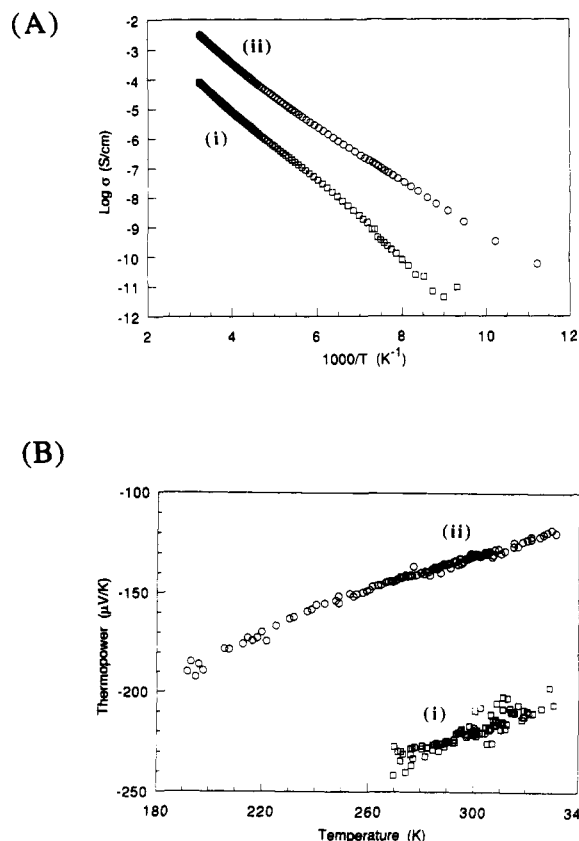**Figure 3.** (A) Four-probe variable-temperature electrical conductivity data of pristine (i) $(PEO)_{0.50}V_2O_5 \cdot nH_2O$ and irradiated (ii) $(PEO)_{0.50}V_2O_5 \cdot nH_2O$ films. (B) Variable-temperature thermoelectric power data of pristine (i) $(PEO)_{0.50}V_2O_5 \cdot nH_2O$ and irradiated (ii) $(PEO)_{0.50}V_2O_5 \cdot nH_2O$ films. Irradiation time was 6 h.

again consistent with the increased number of electron carriers in the former.[13] The thermoelectric power data are shown in Figure 3B.

In summary, $V_2O_5 \cdot nH_2O$ xerogel is an excellent intercalation host for conductive as well as insulating polymers. Poly(ethylene oxide) can be intercalated in $V_2O_5 \cdot nH_2O$ to yield new layered systems with interesting lithium redox intercalation and photochemical properties. The properties of these new PEO/V_2O_5 complexes and their intercalation behavior toward Li^+, as well as intercalation of other insulating polymers in this layered host are under investigation.

Registry No. Lithium, 7439-93-2.

(12) Liu, Y.-J.; Wu, C.-G.; Kanatzidis, M. G.; DeGroot, D. C.; Schindler, J.; Kannewurf, C. R. Manuscript in preparation.

(13) (a) It has been reported that at high water content the conductivity of the $V_2O_5 \cdot nH_2O$ xerogels is primarily protonic particularly near room temperature.[9] Although ionic is less likely for the irradiated $(PEO)_{0.50}V_2O_5 \cdot nH_2O$ films, it may occur in the pristine films. We are currently conducting audio-frequency impedance spectroscopy on these samples to address this point. (b) Liu, Y.-J.; Wu, C.-G.; Kanatzidis, M. G.; DeGroot, D. C.; Schindler, J.; Kannewurf, C. R. Work in progress.